

ESTIMATING THE STRUCTURE OF ${}^6,{}^7\text{Li}$ AT $\sim 4.0\text{A GeV}/c$ BY MOMENTA MEASUREMENTS OF PROJECTILE FRAGMENTS IN EMULSION INTERACTIONS

M. S. EL-NAGDY*, M. M. SHERIF[†], O. WAHBA* and F. A. ABDEL-WAHED*,[‡]

*Physics Department, Faculty of Science, Helwan University, Ein Helwan, Cairo, Egypt

[†]Physics Department, Faculty of Science, Cairo University, Cairo, Egypt

Received 21 February 2005

Revised 28 March 2005

This work presents results on charged state topology of relativistic fragmentation of ${}^6\text{Li}$ and ${}^7\text{Li}$ nuclei at 4.5A and 3.8A GeV/c, respectively, on photoemulsion nuclei. The results would make it possible to answer some topical questions concerning the cluster structure of lithium isotopes. The isotopic composition of fragments and the channels of ${}^6,{}^7\text{Li}$ fragmentation as well as the mean momenta $\rho\beta c$ of projectile fragments have been measured. Yields of ${}^1\text{H}({}^3\text{He})$ appear to have the highest probability due to the fragmentation of ${}^7\text{Li}$, while ${}^2\text{H}({}^4\text{He})$ and ${}^1\text{H}({}^4\text{He})$ are dominant through ${}^6\text{Li}$ -fragmentation process. The presence of exotic ${}^6\text{He}$ among fragmentation process is observed in ${}^7\text{Li}$ with yield 3% while 0.65% were found in ${}^6\text{Li}$.

Keywords: Nuclear physics; ${}^6,{}^7\text{Li}$ structure; projectile fragments; momenta measurements.

1. Introduction

Great progress^{1–4} has been made towards studying the structure of nuclei with excess and maximum number of neutrons while research on the structure of proton-rich (or neutron-deficient) nuclei is merely being planned. The major goal of the appropriate experiment is to define the structural features of nuclei near the boundary of proton stability. Such nuclei are stable in the absence of electron shell. The structure of such nuclei can become another key to understand the process of nucleosynthesis.

In a previous analysis,⁵ a systematic comparison using shower particle distributions of ${}^6\text{Li}$ and ${}^7\text{Li}$ interactions with emulsion nuclei when they participate in the interaction with one ($Z = 1$) or two ($Z = 2$) charged particles, respectively, led to the assumption that ${}^6\text{Li}$ can be considered as a cluster of $(\alpha + d)$, while ${}^7\text{Li}$ may not be $(\alpha + t)$. Here, we report on results from separating hydrogen and helium iso-

[‡]Deceased

topes by using their momentum measurements of ${}^7\text{Li}$ fragments at 3.8A GeV/c in emulsion interactions. The corresponding data for ${}^6\text{Li}$ fragments^{6,7} at 4.5A GeV/c were used for comparison. Branching ratio of fragmentation channels as well as isotope fragment distributions were studied. Information on the ${}^7\text{Li}$ and ${}^6\text{Li}$ structure estimation has been obtained from analyzing the data. Finally, there were a few events including ${}^6\text{He}$ (exotic nuclei), where the (${}^6\text{He} + p$) was one of the dissociation channels of ${}^7\text{Li}$ nuclei.

2. Experimental Method

In this work, the emulsion chamber used was assembled as a stack of Br-2 type emulsion layers having sensitivity up to relativistic particles. Each sheet consists of 600 μm in thickness and dimension $10 \times 20 \text{ cm}^2$. These sheets were horizontally exposed to beams of ${}^6\text{Li}$ and ${}^7\text{Li}$ at momenta of 4.5A and 3.7A GeV/c, respectively, at the JINR synchrophasatron in Dubna. Scanning was carried out by along-the-track method using Leitz Laborlux-S microscope. Each lithium track was carefully followed until it either interacts or leaves the pellicle.

Table 1. Experimental values of average mean free paths (λ_{expt}) in addition to that calculated according to the Bradt–Peters,¹⁶ by using two different overlap parameters from Refs. 17 and 18 in ${}^6\text{Li}$ (4.5A GeV/c), and ${}^7\text{Li}$ (3.8A GeV/c) in comparison with different projectile beams at similar momentum per nucleon.

Projectile	(λ_{expt}) cm	(λ_{cal}) cm	(λ_{cal}^*) cm	Ref.
${}^1\text{H}$	3.2 ± 0.70	32.10	35.15	8
${}^2\text{H}$	26.9 ± 0.60	23.63	23.74	9
${}^3\text{He}$	23.7 ± 0.70	21.22	21.21	10
${}^4\text{He}$	19.5 ± 0.30	19.45	19.66	11
${}^6\text{Li}$	14.4 ± 0.30	17.24	17.13	Present work
${}^7\text{Li}$	15.0 ± 0.40	16.39	16.28	Present work
${}^{12}\text{C}$	13.7 ± 0.10	13.56	13.49	12
${}^{22}\text{Ne}$	9.9 ± 0.30	10.71	10.71	13
${}^{24}\text{Mg}$	9.6 ± 0.20	10.34	10.35	14
${}^{28}\text{Si}$	8.75 ± 0.31	9.69	9.72	15

Through the total scanned length of 353.87 meters of ${}^6\text{Li}$ tracks, we found 2454 events and the experimental mean free path λ_{expt} equals $14.42 \pm 0.29 \text{ cm}$. For the total scanned length of 248.63 meters of ${}^7\text{Li}$ tracks, we found 1647 events with $\lambda_{\text{expt}} = 15.01 \pm 0.37 \text{ cm}$. The values of λ_{expt} for different projectiles (${}^1\text{H}, {}^2\text{H}, \dots, {}^{28}\text{Si}$)^{8–15} presented in Table 1 were compared with the corresponding ones calculated from the inelastic reaction cross-section according to Bradt–Peters formula¹⁶

$$\sigma_i = \pi r_0^2 (A_P^{1/3} + A_T^{1/3} - d)^2.$$

We used here two different overlap parameters to calculate the corresponding mean free paths; one gives λ_{cal} by using $r_0 = 1.46 \pm 0.01$ fm, $d = 1.21 \pm 0.03$ taken from Ref. 17, and the other gives λ_{expt}^* by using $\sigma_i = 109.2(A_P^{0.29} + A_T^{0.29} - 1.3)^2$ mb, obtained by EMU01 collaboration.¹⁸ From Table 1 it may be stated that the calculated values of the average mean free paths and hence the cross-section agree satisfactorily with the experimental results. The results show a power-law behavior with a beam mass number A . The fitting relation is $\lambda = 33.12^{-0.4}A$ cm.

For ${}^7\text{Li}$ we have chosen a sample of 500 inelastic interaction with $Q \geq 0$, we found 347 events having projectile fragments (i.e. they have a total charge of projectile fragments in the forward hemisphere $Q > 0$); among them we found 264 measurable events and excluded 83 events which cannot be measured because of emulsion defects or because of the overlapping of primary or secondary tracks with the marking grid of the emulsion sheet. Similarly, 1390 inelastic events of ${}^6\text{Li}$ include 1040 having PFs; among them 947 were measured⁷ and 93 were excluded. For all detected interactions, the charged secondaries are classified in accordance with the ordinary emulsion methodical criterion:

- (1) Shower track particles (s-particles with multiplicity N_s): singly charged particle (mostly π -meson) with velocity $\beta = v/c \geq 0.7$.
- (2) Grey track particles (g-particles with multiplicity N_g): mostly recoil protons with velocity range of $0.3 \leq \beta < 0.7$.
- (3) Black particles (b-particles denoted by N_b multiplicity): charged particle with $\beta < 0.3$. Grey and black particles are classified together as heavy particles, N_h where $N_h = N_g + N_b$. For more details see Ref. 19.

Projectile fragments PFs: Referred to the spectator nucleons of the projectile with velocity $\approx 0.97c$ emitted within a fragmentation forward cone " θ_c ".²⁰ In this study they are singly- ($Z = 1$) or multiply- ($Z \geq 2$) charged fragments. Taking the present beams momenta, the value of $\theta_c \leq 3^\circ$. The singly-charged fragments emitted with $Z = 1$ are visually separated and identified according to their number of grains per 100 micron when followed up to a distance of ≈ 1 cm from the interaction point without changing its ionization. The PFs of charge $Z \geq 2$ were determined and identified by measuring the grain density, gap density and by δ -ray counting as discussed in Ref. 20. In each event the total charge of non-interacting projectile nucleons $Q = \sum Z_{\text{PFs}}$ was estimated. The multiplicities (average numbers and distributions) of all types of charged secondaries in relativistic ion collisions depend on the average number of interacting projectile nucleons $\langle N_{\text{int}} \rangle$ which is calculated from

$$\langle N_{\text{int}} \rangle = A_P - (A_P/Z_p)Q.$$

The events associated with PFs emitted in the fragmentation cone with charge $Z \geq 1$ represent peripheral collisions at different impact parameters " b " of collision. For all projectile fragments of (264) events of ${}^7\text{Li}$ we have measured momenta quantity ($p\beta c$). The determination of ($p\beta c$) and its error is made through the mea-

surement of multiple Coulomb scattering of the fragments by the Coulomb fields of the emulsion nuclei along the fragment paths, the deviations of their paths were measured by the coordinate method using KSMI Zeiss Jena microscope, and the calculations of $(p\beta c)$ was made by the ρ -method²¹ which takes into account second and third differences of the Y -coordinates of the track to exclude the effect of spurious scattering. We followed the tracks to the maximum possible length and followed some of them from plate to plate to increase the measured length, a unit cell length of 500 μm gives the best precision of our measurements. The corrected mean track deflection $D_{\text{corrected}}$ in the cell length (t) is related with the value $(p\beta c)$ by the relation

$$p\beta c = (k \cdot Z_f \cdot t^{3/2} / (180/\pi) \cdot D_{\text{corrected}}) 10^{-4} \text{ GeV},$$

where Z_f is the charge, p the momentum, k the scattering constant whose numerical value is well known. The statistical error $\Delta(p\beta c)$ (the standard deviation) is obtained from

$$\Delta(p\beta c) = \frac{p\beta c}{\sqrt{N-1}},$$

where N is the number of readings along the scattering track. Details on the momenta measurements method are given in Ref. 22.

3. Results and Discussion

3.1. Multiplicity study

In Table 2, the mean values of multiplicity of s, g, b particles for ${}^6\text{Li}$ and ${}^7\text{Li}$ interactions with emulsion as a function of the Q (non-interacting projectile nucleons) have been presented. There are also $\langle N_{\text{int}} \rangle$ and $\langle N_{\text{int}}^* \rangle$ which can be considered as estimate of a number of inelastic interactions of projectile-nucleus nucleons with target nucleons. The characteristics of the first one was presented in Ref. 5. In Table 2, a group of events with $Q = 0$ is called central or head-on collisions. Events with $Q = 3$ include inelastic interactions with conservation of charge of a projectile nucleus, which contain events with diffractive and electromagnetic dissociation of a projectile nucleus, in addition to events provided by interactions of projectile nucleus neutrons with target nuclei. Events with $Q = 1$ and $Q = 2$ are called peripheral collision at different impact parameters in which charges $Z = 2$ and $Z = 1$ have participated in the collision, respectively.

It is interesting to point out that the values of $\langle N_s \rangle$ for ${}^6\text{Li}$ are found to be higher than the corresponding values of ${}^7\text{Li}$ in all groups of Q values except for $Q = 3$, whereas $\langle N_s \rangle$ and $\langle N_b \rangle$ are slightly higher for ${}^7\text{Li}$. This may be due to the probability of neutron interactions being larger in case of ${}^7\text{Li}$ than ${}^6\text{Li}$ owing to the excess of neutrons in ${}^7\text{Li}$. There is a large difference between the values of $\langle N_b \rangle$ for ${}^6\text{Li}$ and ${}^7\text{Li}$ at $Q = 0$. We attribute this to the fact that the excitation energy given to the target nucleus in central events is larger for ${}^6\text{Li}$. This may also be due to the structures of nucleons in ${}^6\text{Li}$ and ${}^7\text{Li}$. The values of $\langle N_b \rangle$ for all Q 's except

Table 2. The experimental characteristics of ${}^6\text{Li}$ (4.5A GeV/c) and ${}^7\text{Li}$ (3.8A GeV/c) in nuclear emulsion as a function of noninteracting projectile fragments (Q) and mean values of interacting nucleons $\langle N_{\text{int}} \rangle$ in addition to the value $\langle N_{\text{int}}^* \rangle = \langle n_s \rangle$ Li-Em/ $\langle n_s \rangle$ p-Em.

Projectile	$\langle n_s \rangle$	$\langle N_g \rangle$	$\langle N_h \rangle$	$\langle N_{\text{int}} \rangle$	$\langle N_{\text{int}}^* \rangle$
${}^6\text{Li}$	9.4 ± 0.6	5.4 ± 0.3	13.5 ± 0.8	7.0 ± 0.4	6.3 ± 0.4
${}^7\text{Li}$	6.0 ± 0.3	4.9 ± 0.3	9.1 ± 0.5	6.0 ± 0.4	5.8 ± 0.6
${}^6\text{Li}$	6.0 ± 0.4	3.0 ± 0.2	5.6 ± 0.4	4.7 ± 0.3	4.4 ± 0.3
${}^7\text{Li}$	4.2 ± 0.3	3.0 ± 0.2	6.3 ± 0.4	4.0 ± 0.3	3.7 ± 0.4
${}^6\text{Li}$	3.2 ± 0.2	1.5 ± 0.1	3.3 ± 0.2	2.3 ± 0.1	2.3 ± 0.2
${}^7\text{Li}$	2.2 ± 0.1	1.5 ± 0.1	3.2 ± 0.2	2.0 ± 0.1	2.0 ± 0.2
${}^6\text{Li}$	0.8 ± 0.1	0.5 ± 0.0	1.2 ± 0.1	0.5 ± 0.1	1.1 ± 0.1
${}^7\text{Li}$	1.0 ± 0.1	0.7 ± 0.1	2.1 ± 0.2	0.5 ± 0.1	0.5 ± 0.1
${}^6\text{Li}$ $Q = 1.3 \pm 0.1$ total sample	5.1 ± 0.3	4.2 ± 0.2	4.9 ± 0.3	3.4 ± 0.1	3.1 ± 0.8
${}^7\text{Li}$ $Q = 1.3 \pm 0.1$	3.6 ± 0.2	3.8 ± 0.1	5.4 ± 0.2	3.9 ± 0.1	3.8 ± 0.2

$Q = 0$ and 3, and the values of $\langle N_g \rangle$ for the two lithium isotopes are found to be nearly constant within the experimental errors. This reflects the weak dependence of target fragments on the mass number and energy of projectile beam.

A comparison of shower-particle multiplicity distributions for ${}^6\text{Li}$ and ${}^7\text{Li}$ in recent works of ours⁵ for $Z = 1$ ($Q = 2$) participants with original protons at 3.0 GeV/c²³ and 4.5A GeV/c deuterons⁹ have been performed. It may be inferred that $Z = 1$ participants from ${}^7\text{Li}$ are mostly protons, and $Z = 1$ participants from ${}^6\text{Li}$ could be due to a deuteron. The corresponding average values $\langle N_s \rangle$ are equal to 2.17 ± 0.12 and 0.95 ± 0.05 for $Z = 1$ from ${}^7\text{Li}$ and proton, respectively, and 3.2 ± 0.2 , 3.1 ± 0.1 for $Z = 1$ from ${}^6\text{Li}$ and deuteron, respectively. It has been concluded that $Z = 2$ when collided from ${}^6\text{Li}$ and ${}^7\text{Li}$ includes nearly equal amounts of ${}^3\text{He}$ and ${}^4\text{He}$. These results could be obtained from a comparison of shower track multiplicities in lithium events with $Z = 2$ ($Q = 1$) within the corresponding data of 6.0A GeV/c, ${}^3\text{He}$ and 4.5A GeV/c ${}^4\text{He}$.¹⁰ The corresponding average values $\langle N_s \rangle$ are equal to 4.2 ± 0.3 and 6.0 ± 0.4 for $Z = 2$ from ${}^6\text{Li}$ and ${}^7\text{Li}$, respectively and the same are 5.9 ± 0.3 and 5.7 ± 0.1 for ${}^3\text{He}$ and ${}^4\text{He}$, respectively. This may suggest the possibility of clustering ($\alpha + d$) in ${}^6\text{Li}$ nucleus but it may not be ($\alpha + t$) for ${}^7\text{Li}$.

3.2. Momentum study

Table 3 summarizes 30 fragmentation channels obtained from momentum measurement ($p\beta c$) for 264 out of 347 interactions ($Q \geq 0$) having projectile fragments through an examination of 500 unbiased events with ($Q \geq 0$) of ${}^7\text{Li}$ in emulsion nuclei. For comparison the corresponding data obtained from 768 ($Q > 0$) through

Table 3. Fragmentation channels of ${}^6\text{Li}$ and ${}^7\text{Li}$ projectile nuclei.

Projectile PFs particle channel	${}^6\text{Li}$		${}^7\text{Li}$	
	No. of event	% to 768 event ($Q > 0$)	No. of event	% to 264 events ($Q > 0$)
<i>p</i>	90	11.72	38	14.4
<i>pp</i>	23	2.99	13	4.92
<i>ppp</i>	5	0.65	1	0.38
<i>pppp</i>	1	0.13	0	0
<i>d</i>	97	12.63	30	11.36
<i>dp</i>	64	0.88	15	5.68
<i>dpp</i>	8	1.04	0	0
<i>dd</i>	27	3.52	5	1.89
<i>ddp</i>	8	1.04	1	0.38
<i>ddd</i>	3	0.39	0	0
<i>t</i>	32	4.17	5	1.89
<i>tp</i>	24	3.13	2	0.76
<i>tpp</i>	5	0.65	0	0
<i>td</i>	21	2.73	1	0.38
<i>tdp</i>	8	1.04	2	0.76
<i>tt</i>	4	0.52	0	0
${}^3\text{He}$	46	5.99	52	19.69
${}^3\text{He } p$	18	2.34	34	12.88
${}^3\text{He } pp$	1	0.13	0	0
${}^3\text{He } d$	29	3.78	14	5.3
${}^3\text{He } dp$	1	0.13	0	0
${}^3\text{He } t$	8	1.04	4	1.52
${}^4\text{He}$	97	12.63	24	9.09
${}^4\text{He } p$	65	8.64	8	3.03
${}^4\text{He } pp$	4	0.52	0	0
${}^4\text{He } d$	61	7.94	1	0.38
${}^6\text{He}$	5	0.65	3	1.14
${}^6\text{He } p$	0	0.0	5	1.89
${}^6\text{Li}$	13	1.69	6	2.27

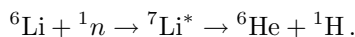
a 947 ($Q \geq 0$) interaction of 4.5A GeV/c ${}^6\text{Li}$ interaction are given in this table. Also, the percentage of each producing channel relative to the number of events having $Q > 0$ are presented. It is clear that 70% of the events contain at least one charged fragment and 22 from 30 channels are nonzero for ${}^7\text{Li}$ (present data) as compared with 80% and 29 channels are nonzero for ${}^6\text{Li}$ (7). The correlation between the yields in different channels for ${}^6\text{Li}$ and ${}^7\text{Li}$ is described as follows:

- (1) For channels of $Q = 1$ and $Z_{\max} = 1$ (i.e. channels of *p*, *d* and *t*), where Z_{\max} is the maximum possible charge on a given projectile fragment there is only one singly-charged particle (*p*, *d* or *t*) emitted as a projectile fragment in the

narrow forward cone and the remaining charged particles ($Z = 2$) collided with emulsion target. The percentage yields of p , d and t are 52%, 41% and 7%, respectively for ${}^7\text{Li}$, and were 41%, 44% and 15%, respectively for ${}^6\text{Li}$ as calculated in Ref. 7.

- (2) For channels of $Q = 2$ and $Z_{\max} = 1$ [i.e. channels of (pp) , (dp) , (dd) , (tp) , (td) and (tt)]: two singly-charged particles are emitted as projectile fragments leaving the remaining singly-charged particles to interact with the target nucleus. The percentage yields of p , d and t in these channels are $\sim 60\%$, 36% and 4% for ${}^7\text{Li}$ and are 41%, 43% and 16%, respectively for ${}^6\text{Li}$.
- (3) For channels of $Q = 2$, $Z_{\max} = 2$, [i.e. the channels of $({}^3\text{He})$, $({}^4\text{He})$ and $({}^6\text{He})$], the doubly-charged ions are emitted as projectile fragments while the remaining singly-charged particles interacting with the target nucleus. The percentage yields of ${}^3\text{He}$; ${}^4\text{He}$ and ${}^6\text{He}$ are $\sim 66\%$, 30% and 4% for ${}^7\text{Li}$ and are 31%, 66% and 3%, respectively for ${}^6\text{Li}$.
- (4) For channels of $Q = 3$ and $Z_{\max} = 1$, [i.e. channels of (ppp) , (dpp) , (ddp) , (ddd) , (tpp) and (tdp)], the three charged particles are emitted as projectile fragments. In these channels, the percentage yields of p , d and t are $\sim 50\%$, 33% and 17% for ${}^7\text{Li}$ and are $\sim 51\%$, 37% and 12% , respectively for ${}^6\text{Li}$.
- (5) For channels of $Q = 3$ and $Z_{\max} = 2$ [i.e. channels of $({}^3\text{He } p)$, $({}^3\text{He } d)$, $({}^3\text{He } t)$, $({}^4\text{He } p)$, $({}^4\text{He } d)$, $({}^4\text{He } t)$ and $({}^6\text{He } p)$], the projectile nucleus is fragmented into one singly-charged particle associated with a doubly ionized helium isotope. The percentage yields of p , d and t in these channels are $\sim 71\%$, 23% and 6% for ${}^7\text{Li}$ and are $\sim 46\%$, 50% and 4% , respectively for ${}^6\text{Li}$. The percentages of ${}^3\text{He}$, ${}^4\text{He}$ and ${}^6\text{He}$ in these channels are $\sim 79\%$, 14% , 7% for ${}^7\text{Li}$ and are $\sim 30\%$, 70% and 0% , respectively for ${}^6\text{Li}$.
- (6) For channels of $Q > 3$ and $Z_{\max} = 1$ or 2 : i.e. $(pppp)$ 0.13%, $({}^3\text{He } pp)$ 0.13%, $({}^3\text{He } dp)$ 0.13% and $({}^4\text{He } pp)$ 0.52%, the charge conservation is violated in these channels and appears only among ${}^6\text{Li}$ fragmentation channels⁷ but not among ${}^7\text{Li}$ channels. This means that there are a few cases of pion exchange or nucleon pick-up by ${}^6\text{Li}$ projectile nuclei from target nuclei.

It can be seen from Table 3 that the fractions of two isotopes ${}^3\text{He } p$ are more abundant in the fragmentation channels of ${}^7\text{Li}$ while enrichment of ${}^4\text{He } d$ and ${}^4\text{He } p$ were observed for ${}^6\text{Li}$ fragmentation. The fraction of (t) exceeds in ${}^6\text{Li}$ than that in ${}^7\text{Li}$ by a factor of more than -2 for channels of $Q = 1$ or 2 and $Z_{\max} = 1$. In case of $Q = 3$ and $Z_{\max} = 1$ or 2 , t exceeds by a factor of about 1.5 for ${}^7\text{Li}$ than ${}^6\text{Li}$, as follows: For presence of the isotope ${}^6\text{He}$ among the doubly charged fragments, there is some enhancement in ${}^7\text{Li}$ (eight events out of 264 with percentage of 3%), while five events out of 768 with 0.65% were found in ${}^6\text{Li}$. The observation of ${}^6\text{He}$ among the doubly charged fragments of ${}^7\text{Li}$ and ${}^6\text{Li}$ comes as a surprise. It can be produced via charge exchange between the projectile and target nucleons in ${}^6\text{Li}$



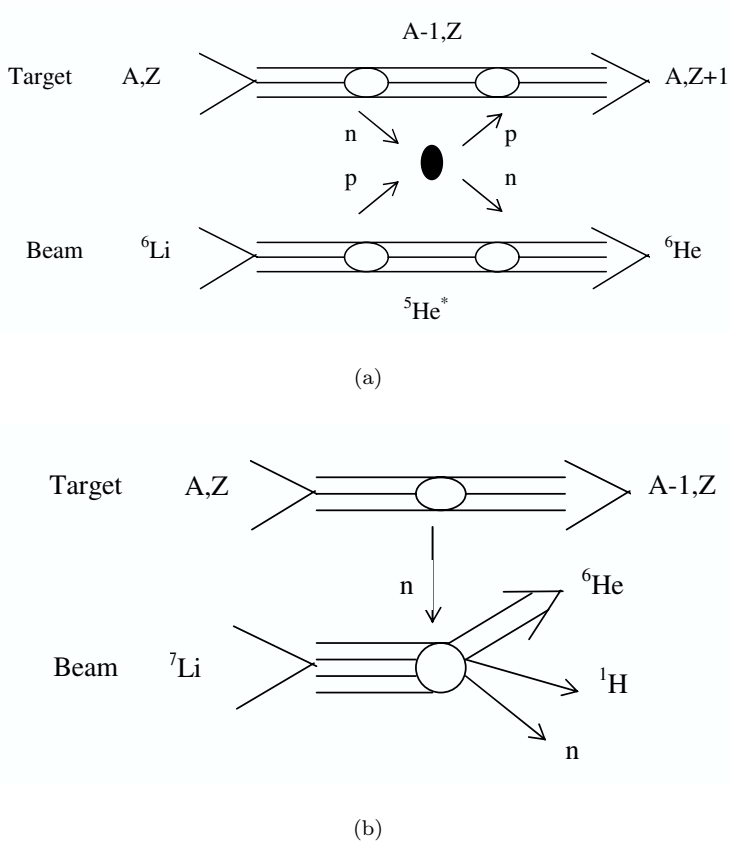


Fig. 1. Diagrams corresponding to events involving the charge exchange to produce (a) ${}^6\text{He}$ from ${}^6\text{Li}$, (b) ${}^6\text{He}$ from ${}^7\text{Li}$ by direct breakup.

In ${}^7\text{Li}$, it is produced through direct break up of ${}^7\text{Li}$ into two fragments ${}^7\text{Li} \rightarrow {}^6\text{He} + {}^1\text{H}$ (five events were observed) even with or without evidence of excitation of the target nucleus, in addition to this three events were found due to fragmentation of ${}^7\text{Li}$ into ${}^6\text{He}$, leading thus a proton to make inelastic interaction inside the emulsion nucleus. Figure 1 shows a diagram of producing ${}^6\text{He}$ in the interactions of ${}^6\text{Li}$ and ${}^7\text{Li}$ with target nuclei.

Figures 2 and 3 show the separation of the hydrogen and helium isotopes using $p\beta c$ measurements. The data are shown by histograms, and the curves represent Gaussian fitting. In Fig. 2 there is a distribution of 223 singly-charged relativistic track particles with region of $2 < p\beta c < 13$ GeV/c, with peaks at 3.8, 7.5 and 11.7 GeV/c corresponding to isotopes ${}^1\text{H}$, ${}^2\text{H}$, ${}^3\text{H}$, respectively. In Fig. 3 the distribution of 143 doubly-charged track particles with region of $10 < p\beta c < 23$ GeV/c is shown, with peaks at ~ 11.7 , 15.2 and 21.5 GeV/c corresponding to isotopes ${}^3\text{He}$, ${}^4\text{He}$ and ${}^6\text{He}$, respectively. The results of all isotopes are summarized in Table 4. For comparison, the corresponding data^{6,7} obtained from ${}^6\text{Li}$ are also listed in Table 4.

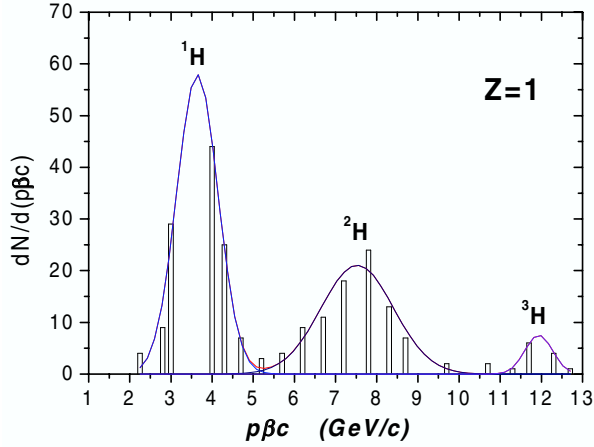


Fig. 2. Separation of hydrogen isotopes in ^7Li fragments using $p\beta c$ measurements. The curves represent the Gaussian distribution, best fit.

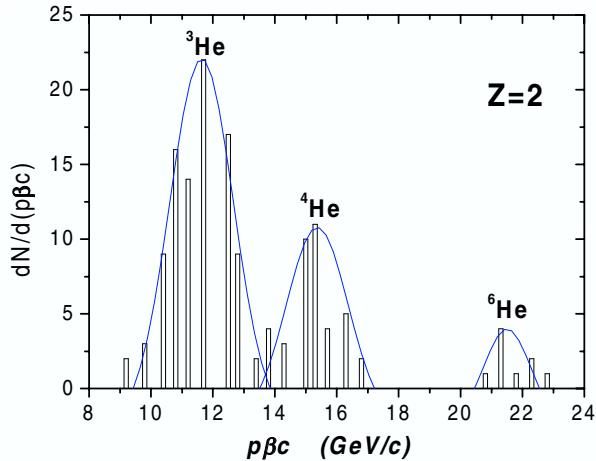


Fig. 3. Separation of helium isotopes in ^7Li fragments using $p\beta c$ measurements. The curves represent the Gaussian distribution, best fit.

Moreover, it can be seen from Table 4 that:

- (a) For singly-charged isotopes p , d , t one can find a higher yield of protons (60%) and 34% and 6% for deuteron and triton, respectively. On the other hand, the yields of p , d and t are practically equal in both experiments of ^6Li fragmentation with values around $\sim 45\%$ for each of p and d and 10% for triton.
- (b) For doubly-charged isotopes ^3He , ^4He and ^6He in ^7Li the high yield of ^3He (72%) is observed with 22% for ^4He and 6% for ^6He . In ^6Li the relative yields of ^3He and ^4He are approximately equal as given in Ref. 6 with values 51 and

Table 4. Yields of fragments isotopes from ${}^7\text{Li}$ compared with those of ${}^6\text{Li}$ projectile nuclei.

Isotope	Ratio %		
	${}^6\text{Li}$ Ref. 6	${}^6\text{Li}$ Ref. 7	${}^7\text{Li}$ Present work
p	47 ± 2	44 ± 7	60 ± 5
d	46 ± 2	43 ± 7	34 ± 4
t	7 ± 1	13 ± 3	6 ± 2
${}^3\text{He}$	51 ± 2	30 ± 7	72 ± 7
${}^4\text{He}$	46 ± 2	68 ± 8	22 ± 4
${}^6\text{He}$	3 ± 1	1.4 ± 0.3	6 ± 2

46 respectively. They differ in Ref. 7 (30 and 68%). Moreover, an almost equal ${}^3\text{He}$ and ${}^4\text{He}$ yields close to these values were obtained by Greiner *et al.*²⁴ in the fragmentation of relativistic ${}^{12}\text{C}$ and ${}^{16}\text{O}$.

- (c) Referring to ${}^6\text{He}$, its fraction in ${}^7\text{Li}$ exceeds that of ${}^6\text{Li}$ by a factor of 2 or more as given in Refs. 6 and 7. This leads to the conclusion that proton yields dominate the singly-charged fragments in ${}^7\text{Li}$ -fragmentation process while proton and deuteron yields are approximately equal in ${}^6\text{Li}$ -fragmentation process. Also ${}^3\text{He}$ fragments are dominant on doubly-charged fragments in ${}^7\text{Li}$ -fragmentation process, while ${}^4\text{He}$ yields are the dominant doubly-charged fragments in ${}^6\text{Li}$ -fragmentation process. More ${}^6\text{He}$ are produced in the fragmentation of ${}^7\text{Li}$ than that of ${}^6\text{Li}$.

Table 5 shows the dissociation channels⁷ of ${}^7\text{Li}$ and ${}^6\text{Li}$ with events of type ($Q = 3$). These events are classified into two categories according to the number of heavy target fragments ($N_h = 0$ and $N_h > 0$). The events of $N_h = 0$ represent pure Coulomb-dissociation events. These events are very sensitive probe to the structure of the projectile nucleus because it contains only the projectile constituent nucleons. The group of events with $N_h > 0$ represent inelastic interactions of ${}^{6,7}\text{Li}$ with a target in which the projectile charge is conserved. In these events one or more neutrons have collided. It can be observed from Table 5 that:

- (a) In ${}^7\text{Li}$ the highest probability (34 events) with $N_h = 0$ and $N_h > 0$ with percentage (49%), ${}^7\text{Li}$ nuclei split into two fragments ${}^7\text{Li} \rightarrow {}^3\text{He} + p + 3n$. There are probabilities for 20% (${}^3\text{He}, d, 2n$), 11% (${}^4\text{He}, p, 2n$), 7% (${}^6\text{He}, p$) and 6% (${}^3\text{He}, t$), noted here.
- (b) ${}^6\text{Li}$ 74 events (77%) corresponding to splitting of ${}^6\text{Li}$ nuclei into ${}^4\text{He}, d$, 12% (tdp) and 8% (${}^3\text{He} t$).
- (c) The fragmentation behavior of both ${}^7\text{Li}$ and ${}^6\text{Li}$ nuclei keeps the same trend independent of the N_h values.

Table 5. Channels of dissociations of ${}^7\text{Li}$ compared with ${}^6\text{Li}$ for events having $Q = 3$ with $N_h = 0$ and $N_h > 0$.

Dissociation channel	${}^7\text{Li}$ present work			${}^6\text{Li}$		
	$N_h = 0$	$N_h > 0$	Total	$N_h = 0$	$N_h > 0$	Total
<i>ppp</i>	—	1	1	—	—	—
<i>ddp</i>	—	1	1	—	—	—
<i>ddd</i>	—	—	—	—	2	2
<i>tdp</i>	2	—	2	4	3	7
${}^3\text{He } p$	18	16	34	—	—	—
${}^3\text{He } d$	10	4	14	—	—	—
${}^3\text{He } t$	2	2	4	4	1	5
${}^4\text{He } p$	5	3	8	—	—	—
${}^4\text{He } d$	1	—	1	23	24	47
${}^6\text{He } p$	2	3	5	—	—	—

4. Conclusion

We have reported the momenta measurements of fragments obtained from the fragmentation of relativistic ${}^7\text{Li}$ with momentum $3.8\text{A GeV}/c$ in photoemulsion nuclei. The isotopic composition of fragments and the channels of ${}^7\text{Li}$ fragmentation are determined and compared with those obtained from ${}^6\text{Li}$ fragmentation at $4.5\text{A GeV}/c$. The results obtained from this study allow one to make the following conclusions:

- (1) Yields of hydrogen isotopes are ($\approx 60\%$ protons, 34% deuterons, and 6% tritons) and helium isotopes are ($\approx 72\%$ ${}^3\text{He}$, 22% ${}^4\text{He}$, and 6% ${}^6\text{He}$) for ${}^7\text{Li}$ and are ($\approx 47\%$ protons, 46% deuterons and 7% tritons) and (51% ${}^3\text{He}$, 46% ${}^4\text{He}$, 3% ${}^6\text{He}$) respectively for ${}^6\text{Li}$.
- (2) There is a higher probability of splitting events into two charged fragments for ${}^3\text{He } p$ for ${}^7\text{Li}$ and ${}^4\text{He } p$ and ${}^4\text{He } d$ for ${}^6\text{He}$.
- (3) Enhancement of isotope ${}^6\text{He}$ among fragmentation of ${}^7\text{Li}$ ($\sim 3\%$) is observed through direct breakup while it is 0.65% in ${}^6\text{Li}$ through charge exchange between the projectile and target.
- (4) In ${}^7\text{Li}$ events of coherent dissociation in which the projectile charge is conserved with $N_h \geq 0$, the results are (49% ${}^3\text{He} + p + 3n$, 20% ${}^3\text{He}, d, 2n$, 11% ${}^4\text{He}, p, 2n$, 7% ${}^6\text{He}, p$, 6% ${}^3\text{He}, t, n$) and 77% ${}^4\text{He}, d$, 12% *tdp*, 8% ${}^3\text{He } t$ for ${}^6\text{Li}$. These fragmentation behavior keeps the same trend independent of the N_h values.

References

1. P. G. Hansen and A. S. Jensen, *Ann. Rev. Nucl. Part. Sci.* **45**, 591 (1995), Introduction.
2. A. H. Wuosamaa, R. R. Betts, M. Freer and B. R. Fulton, *Ann. Rev. Nucl. Part. Sci.* **45**, 89 (1995), Introduction.
3. W. Schwab *et al.*, *Z. Phys.* **A350**, 283 (1995).

4. M. H. Semdberg *et al.*, *Phys. Lett.* **B452**, 1 (1999).
5. M. El-Nadi *et al.*, in *Proc. of Int. Sch. of Cosmic Ray Astrophysics*, 10th Course, Erice, Italy, 1996.
6. F. G. Lepekhin, D. M. Seliverstov and B. B. Simonov, *Eur. Phys. J.* **A1**, 137 (1998).
7. M. I. Adamovich, V. G. Bogdanov, I. A. Konorov, V. G. Larionova, N. G. Peresadko, V. A. Plyushchev, Z. I. Solovyeva and S. P. Kharlamov, *Phys. Ato. Nucl.* **62**, 8; 1378 (1999).
8. V. I. Bubnov *et al.*, *Z. Phys.* **A303**, 133 (1981).
9. M. I. Adamovich *et al.*, preprint JINR, E1-10838 Dubna (1977); A. El-Naghy and V. D. Toneev, *Z. Phys.* **A298**, 55 (1980).
10. M. M. Sherif and M. Mohery, *Egypt J. Phys.* **22**, 1; 125 (1991).
11. M. El-Nadi, M. M. Sherif, M. S. El-Nagdy, A. Abdelsalam, M. N. Yasin, M. A. Jilany and A. Bakr, *Int. J. Mod Phys.* **E2**, 381 (1993).
12. M. El-Nadi, O. E. Badawy, A. Moussa, E. Khalil and A. Hamalawy, *Phys. Rev. Lett.* **52**, 1971 (1984).
13. B. P. Bannik *et al.*, *Sov. J. Nucl. Phys.* **52**, 982 (1984).
14. S. El-sharkawy, M. K. Hegab, O. M. Osman and M. A. Jilany, *Phys. Script.* **47**, 512 (1993).
15. M. A. Jilany, *Nucl. Phys.* **A579**, 627 (1994).
16. H. L. Bradt and B. Peters, *Phys. Rev.* **77**, 54 (1950).
17. E. O. Abdrkhmanov *et al.*, **C5**, 1 (1980); N. Angelov *et al.*, *Sov. J. Nucl. Phys.* **33**, 552 (1981).
18. EMUO1-Collab. (M. I. Adamovich *et al.*), Lund Univ. Report Nos. LUIP 8904, 8906, 8907 (1989).
19. M. S. El-Nagdy, A. Abdelsalam, N. Ali-Mossa, A. M. Abdalla, S. M. Abdal-Halim and K. Abdel-Waged, *Nucl. Phys.* **A730**, 419 (2004).
20. M. El-Nadi, M. S. El-Nagdy, N. Ali-Mossa, A. Abdelsalam, A. M. Abdalla and A. A. Hamed, *J. Phys.* **G25**, 1169 (1999).
21. V. G. Voinov and I. Ya. Chasnikov, *Mnogokratnoe Rasseyanie Chastits U Yadernych Fotoemul'siyakh (Particle Rescattering in Nuclear Photoemulsions)* (Nauka, 1969), p. 81.
22. C. F. Powell, P.H. Fowler and D. H. Perkins, *The Study of Elementary Particles by the Photographic Method* (Pergamon Press, 1959).
23. M. Bagdanski *et al.*, *Helv. Phys. Acta.* **42**, 485 (1969).
24. D. E. Greiner *et al.*, *Phys. Rev. Lett.* **35**, 152 (1975).